arXiv:1512.05618v2 [hep-ph] 7 Apr 2016

Diphoton Excess at 750 GeV from a Radion in the Bulk-Higgs Scenario

Peter Cox[a,1], Anibal D. Medina[b,2],
Tirtha Sankar Ray[c,3] and Andrew Spray[d,4]

[a] *ARC Centre of Excellence for Particle Physics at the Terascale, School of Physics, The University of Melbourne, Victoria 3010, Australia*
[b] *Institut de Physiqué Théorique, Université Paris Saclay, CNRS, CEA, F-91191 Gif-sur-Yvette, France*
[c] *Department of Physics and Center for Theoretical Studies, Indian Institute of Technology, Kharagpur 721302, India*
[d] *Center for Theoretical Physics of the Universe, Institute for Basic Science (IBS), Daejeon, 34051, Korea*

Abstract

In this work we point out that the diphoton excess recently presented by the ATLAS and CMS collaborations might originate from a radion in the bulk Higgs scenario within a warped extra dimension. In this case the couplings of the radion to massive gauge bosons are suppressed, allowing it to evade existing searches. In the presence of mixing with the Higgs, due to the strong constraints from diboson searches, only points near what we denominate the alignment region are able to explain the diphoton signal and evade current experimental constraints. The radion always has a sizeable branching ratio into top pairs, which provides a somewhat model independent channel to probe this scenario in the near future. If alignment is strong however, there are regions of parameter space where diHiggs decays may dominate providing stronger constraints and interesting perspectives for future collider searches.

1 Introduction

Recently the ATLAS and CMS collaborations have reported a mild excess in the diphoton channel around an invariant mass of 750 GeV, with a few fb^{-1} of data and collisions at $\sqrt{s} =$ 13 TeV [1,2]. Though it currently remains uncertain whether this is compatible with a large or narrow width resonance (ATLAS seems to prefer a somewhat broad resonance with $\Gamma \approx 45$ GeV while CMS obtains a better fit with a narrower width), these events do not seem to come along with other particles. Furthermore, the absence of a significant signal in the previous run of the LHC at $\sqrt{s} = 8$ TeV may favour certain production modes. This observation has already inspired a number of theoretical investigations [3, 4].

[1] pcox@physics.unimelb.edu.au
[2] anibal.medina@cea.fr
[3] tirthasankar.ray@gmail.com
[4] a.spray.work@gmail.com

In this work we advance an explanation of the observed excess in the context of warped extra dimensional models via the production of a spin-0 excitation of the metric: the radion, which becomes massive once the metric is stabilized. Similarly, via the AdS/CFT correspondence the radion can be thought of as the pseudo-Nambu-Goldstone boson (pNGB) of the spontaneously broken conformal sector; the dilaton. Warped extra dimensions [5] with the non-factorizable AdS_5 space are a popular setup to address the gauge hierarchy problem and are a practical tool to study strongly coupled conformal sectors via the duality language. In order to explain the diphoton excess we find it advantageous to consider the Higgs field responsible for electroweak symmetry breaking as a *5D* scalar in the *bulk* of the extra dimension. It was shown in Ref. [6] that the coupling of the radion to the massive gauge bosons is then highly suppressed compared to the case of a brane-localized Higgs. This suppresses the radion decay width to WW and ZZ, allowing a relatively light radion to avoid the stringent LHC constraints from diboson searches. In the 4D CFT language, a bulk Higgs corresponds to a generic composite scalar. Spontaneous symmetry breaking driven by a brane-localised potential corresponds to this scalar gaining a VEV only when the CFT runs to the IR. The fine-tuning of the electroweak sector is no worse than for a conventional brane-localised Higgs.

In this paper we first briefly review the radion phenomenology in the bulk Higgs scenario. We demonstrate that limits from 8 TeV resonance searches and measurements of the 125 GeV Higgs already constrain the radion-Higgs mixing to be small, before presenting the region in parameter space that can be in consonance with the observed diphoton excess. We also point out that such a state would have large branching ratios to ditop and digluon final states, possibly in addition to di-Higgs, which provide complementary probes to explore this explanation for the diphoton excess.

2 The Model

The 5D metric for a slice of AdS_5 with boundaries at $y = 0$ (UV-brane) and $y = L$ (IR-brane) is given by,

$$ds^2 = e^{-2ky}\eta_{\mu\nu}dx^\mu dx^\nu - dy^2\,, \tag{1}$$

where y is the extra spatial coordinate and k is the curvature scale. The spin-0 fluctuations of the metric are given by,

$$ds^2 = e^{-2ky-2F(x,y)}\eta_{\mu\nu}dx^\mu dx^\nu - (1+2F(x,y))^2 dy^2\,. \tag{2}$$

The extra dimension also needs to be stabilized, which can be accomplished by the introduction of a scalar sector that couples minimally to gravity and leads to a non-vanishing mass for the radion. In the small back-reaction limit, the physical radion field[5] has an approximate profile of the form [7],

$$F(x,y) \equiv e^{2(ky-kL)}\frac{1}{\Lambda_r}\hat{r}(x)\,, \tag{3}$$

[5]Which is a linear combination of the radion and the scalar introduced to stabilized the extra dimension.

where Λ_r sets the strength of the coupling to Standard Model fields. In the minimal RS model it is related to the 5D Planck mass, M_5, via $\Lambda_r = \sqrt{3M_5^3/k}\, e^{-kL}$. If we treat the RS framework simply as a tool to analyze a 4D CFT, then M_5 and hence kL and Λ_r are free parameters. We discuss the implications of different choices after identifying the best fit values to the 750 GeV excess.

The radion phenomenology has been extensively studied in the case that the Higgs scalar is localized on the IR brane. Here we will consider a bulk Higgs scenario given by the following 5D action

$$S = \int_0^L d^5x\, \sqrt{g} \left[\left(\frac{M_5^3}{2} + \xi H^\dagger H \right) R_5 + |D_M H|^2 - V(H) \right] + S_{brane}\,, \tag{4}$$

where the bulk radion-Higgs mixing is parameterized by ξ. We assume that the bulk and UV brane potentials are renormalizable and that the IR brane potential spontaneously breaks electroweak symmetry. Because the symmetry breaking takes place on the IR brane, the natural size of the 4D VEV is $\tilde{k} \equiv k e^{-kL} \sim \frac{1}{3} m_{KK}$, where m_{KK} is the typical mass of the Kaluza-Klein (KK) resonanaces. This is the same as for a brane-localized Higgs with a tree-level potential, and implies a similar degree of fine-tuning, $v_{ew}^2/\tilde{k}^2 \sim \mathcal{O}(1)\%$, with $v_{ew} = 246$ GeV. Once we fine-tune the Higgs VEV, the Higgs mass is automatically of the same scale and no additional tuning is required.

It was shown in [6] that once the Higgs is promoted to a 5D scalar field and detached from the IR brane into the bulk of the extra dimension, the radion phenomenology can change drastically. In particular, the radion couplings to the Higgs field and the massive gauge bosons are substantially modified compared to the more usual brane-Higgs scenario. Focusing on the coupling to massive SM gauge bosons and expanding the metric in its spin-0 fluctuations in the matter action we obtain

$$\begin{aligned} \mathcal{S}_{matter} &= \int d^4x dy \sqrt{g}\, (D_\mu H^\dagger D^\mu H) \\ &= \int d^4x dy\, e^{-4(A(y)+F(x,y))} (1 + 2F(x,y)) e^{2(A(y)+F(x,y))} D_\mu H^\dagger D^\mu H \\ &\approx \int d^4x dy\, (1 - 4F^2(x,y) + \mathcal{O}(F(x,y)^3)) e^{-2A(y)} D_\mu H^\dagger D^\mu H\,, \end{aligned} \tag{5}$$

where in the last two lines indices are contracted using the Minkowski metric. We therefore see that the linear coupling of the radion to the gauge boson mass terms vanishes. Notice that this is a general result for the kinetic term of any scalar. It is a geometrical result from the 5D point of view, and holds even in pure AdS_5 space (without UV/IR branes) [6]. We can also understand this result through the 4D dual picture, where the dilaton can only couple derivatively to conformally invariant operators. The gauge boson mass terms arise from the Higgs kinetic term, $D_\mu H D^\mu H$, where H is the SM Higgs doublet. Lorentz invariance forbids a linear derivative radion coupling to this operator, and therefore at tree-level the radion only couples to the kinetic terms of the massive gauge bosons. We summarize the other radion couplings in Table 1.

SM final state	Radion coupling
$f\bar{f}$	$\frac{m_f}{\Lambda_r}$
WW	$-\frac{2}{\Lambda_r}\frac{1}{kL}$
ZZ	$-\frac{1}{\Lambda_r}\frac{1}{kL}$
hh	$\frac{1}{\Lambda_r}\left(2m_h^2 - \frac{c_1}{2}m_r^2\right)$
$\gamma\gamma$	$-\frac{1}{\Lambda_r}\left(\frac{1}{kL} + \left[b_{QED} - F_1(\tau_{W,r}) - \frac{4}{3}F_{1/2}(\tau_{t,r})\right]\frac{\alpha_{EM}}{2\pi}\right)$
gg	$-\frac{1}{\Lambda_r}\left(\frac{1}{kL} + \left[b_{QCD} - \frac{1}{2}F_{1/2}(\tau_{t,r})\right]\frac{\alpha_3}{2\pi}\right)$

Table 1: Couplings of the radion in the gauge basis adopted from Ref [6].

As a pNGB, it's possible for the radion to be naturally lighter than the KK resonances [8], which tend to lie in the few TeV range. Therefore, from a purely 4D effective field theory perspective, we can consider simply the SM with an additional scalar. The effective Lagrangian for the Higgs-radion fields, including a bulk mixing term $\xi R_5 H^\dagger H$ and the leading back-reaction contribution, is given by [6]

$$\begin{aligned}\mathcal{L}_{eff} = &\frac{1}{2}\partial_\mu\hat{h}(x)\partial^\mu\hat{h}(x) - \frac{1}{2}m_h^2\hat{h}(x)^2 + \frac{1}{2}\left(1 + c_2\frac{v_{ew}^2}{\Lambda_r^2}\right)\partial_\mu\hat{r}(x)\partial^\mu\hat{r}(x) \\ &- \frac{1}{2}m_r^2\hat{r}(x)^2 - c_1\frac{v_{ew}}{\Lambda_r}\partial_\mu\hat{h}(x)\partial^\mu\hat{r}(x) - c_3\frac{v_{ew}}{\Lambda_r}m_r^2\hat{h}(x)\hat{r}(x)\,,\end{aligned} \tag{6}$$

where c_1, c_2 and c_3 are $\mathcal{O}(1)$ numerical coefficients and $\hat{h}(x)$ is the Higgs scalar. The c_i can in principle be given in terms of wavefunction overlap integrals, but are model-dependent on the details of the radion stabilization.

As is clear from Eq. (6), there is kinetic and mass mixing between the radion and the Higgs. One can diagonalize the kinetic term by going to a new basis

$$\hat{h} = h' + c_1\frac{v_{ew}}{\Lambda_r}\frac{r'}{Z}\,, \qquad \hat{r} = \frac{r'}{Z}\,, \tag{7}$$

where $Z^2 = 1+(c_2+c_1^2)v_{ew}^2/\Lambda_r^2$. This transformation decouples the kinetic mixing but introduces additional mass mixing terms. The mass matrix in the basis (r', h') then takes the form:

$$M = \begin{pmatrix} \frac{m_r^2}{Z^2} + \frac{1}{Z^2}\frac{v_{ew}^2}{\Lambda_r^2}(c_1^2m_h^2 + 2c_1c_3m_r^2) & \frac{1}{Z}\frac{v_{ew}}{\Lambda_r}(c_1m_h^2 + c_3m_r^2) \\ \frac{1}{Z}\frac{v_{ew}}{\Lambda_r}(c_1m_h^2 + c_3m_r^2) & m_h^2 \end{pmatrix}\,. \tag{8}$$

An additional unitary transformation brings us to the mass basis (r, h), where r (h) is the 750 GeV radion-like (125 GeV Higgs-like) field. We can define the relation between the gauge and mass bases as

$$\hat{r}(x) = c_{rr}\,r(x) + c_{rh}\,h(x)\,, \qquad \hat{h}(x) = c_{hr}\,r(x) + c_{hh}\,h(x)\,. \tag{9}$$

Final State	Observed Bound
$t\bar{t}$	< 300 fb [11]
WW	< 38 fb [12, 13]
ZZ	< 12 fb [14]
$Z\gamma$	< 4.0 fb [15, 16]
$\gamma\gamma$	< 1.4 fb [17, 18]
hh	< 36 fb [19]
jj	< 2.5 pb [20, 21]

Table 2: Constraints on the radion from 8 TeV resonance searches.

Note that because of the non-unitary transformation, $c_{ih}^2 + c_{ir}^2 \neq 1$ for $i = h, r$. However, this definition is useful to determine the couplings in the mass basis. In fact, notice that c_{hr} and c_{rh} provide respectively the SM Higgs-like and radion-like couplings of the heavier and lighter mass eigenstates $r(x)$ and $h(x)$, and moreover due to the non-unitarity transformation among the different basis, $c_{hr} = 0$ does not imply that $c_{rh} = 0$ and vice versa.

3 The Diphoton Excess

We use the best-fit cross sections for the diphoton excess from the CMS combined 8+13 TeV analysis [10] and extracted from the ATLAS analysis [1] in Ref. [3]:

$$\mu_{13\ \mathrm{TeV}}^{\mathrm{ATLAS}} = \sigma(pp \to S)_{13\ \mathrm{TeV}} \times \mathcal{B}(S \to \gamma\gamma) = 10^{+4}_{-3}\ \mathrm{fb}, \tag{10}$$

$$\mu_{13\ \mathrm{TeV}}^{\mathrm{CMS}} = \sigma(pp \to S)_{13\ \mathrm{TeV}} \times \mathcal{B}(S \to \gamma\gamma) = 3.7^{+1.5}_{-1.3}\ \mathrm{fb}. \tag{11}$$

We also summarise in Table 2 the most important constraints from 8 TeV resonance searches. The radion couplings to light fermions are suppressed by the fermion mass and so set no meaningful constraints.

From Table 2, we see that the constraints on a putative 750 GeV resonance decaying to gauge bosons are an order of magnitude stronger than on decays to $t\bar{t}$. In contrast, a scalar of that mass with Higgs-like couplings will dominantly decay to WW and ZZ. This has important consequences for our model since the radion and the Higgs generically have both mass and kinetic mixing, as shown in Eq. (6). In order to sufficiently suppress the heavier state decay to gauge bosons, it must be radion-like with any Higgs-like couplings strongly suppressed. Large mixing between the two states would also modify the properties of the 125 GeV scalar resonance discovered at the LHC. Decays of the heavier state to hh could also affect the Higgs measurements, however this contribution will turn out to be negligible in the viable regions of parameter space.

With the radion couplings to massive gauge bosons suppressed, inspecting Table 1 reveals that the other potentially large couplings are to gluons (due to the QCD anomaly), to top-quark pairs (since they are the heaviest SM fermion), and to the lighter Higgs-like state. The decay $r \to t\bar{t}$ is enhanced over $r \to hh$ by colour and spin degrees of freedom, enough that the former

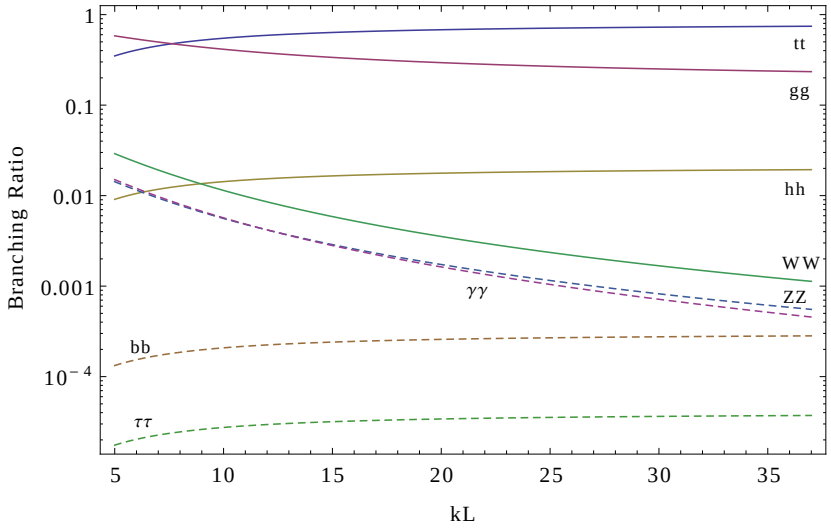

Figure 1: Branching ratios for a 750 GeV radion to various SM final states. This is for the bulk Higgs setup in the zero mixing limit with the SM Higgs.

typically sets the dominant limits despite the stronger constraints on hh final states listed in Table 2. Note from Table 1 that all radion couplings scale with Λ_r in the same way. Therefore in the zero-mixing limit the branching ratios depend only on the size of the extra dimension kL. We plot those in Figure 1, and see that $\mathcal{B}(r \to t\bar{t}) \approx 40\,\mathcal{B}(r \to hh)$.

Our model contains only four free parameters: Λ_r, kL, c_1 and c_3. The observed masses for the Higgs and the diphoton excess fix m_r, m_h in terms of these parameters, while c_2 has a negligible effect since it comes with an additional v_{ew}/Λ_r supression factor. In order to identify the regions of parameter space which both satisfy the current experimental bounds and are consistent with the observed diphoton excess we peform a scan over these parameters. We take flat priors in the range $-2 \leq c_1, c_3 \leq 2$, $5 \leq kL \leq 35$ and $1 \leq \Lambda_r \leq 5\,\text{TeV}$ and require that the 750 GeV state satisfy the constraints from the resonance searches in Table 2, while the 125 GeV state is consistent with the measured Higgs signal strengths [23] at the 2-sigma level. The radion production cross sections are obtained by scaling the Higgs 8 TeV cross section [22] by the radion effective coupling to gluons and, for $\sqrt{s} = 13$ TeV, by the parton luminosity ratio:

$$\frac{\sigma(pp \to r)_{13\ \text{TeV}}}{\sigma(pp \to r)_{8\ \text{TeV}}} \approx 4.7\,. \tag{12}$$

The results of the scan are shown in Figure 2, where all points satisfy the current experimental constraints and the green points are also consistent with the observed diphoton excess. In the left panel we have plotted the 750 GeV component of the Higgs gauge state, c_{hr}, as a function of kL, clearly showing that the current data already enforces small Higgs-radion mixing. Remember that c_{hr} gives a measure of how much Higgs-like couplings the heavier eigenstate possesses, and that for $c_{hr} \approx 0$ the heavier eigenstate has vanishing Higgs-like couplings. Large mixing is immediately excluded by measurements of the 125 GeV state; however it turns out that for much of the parameter space resonance searches in the ZZ and WW final states provide the

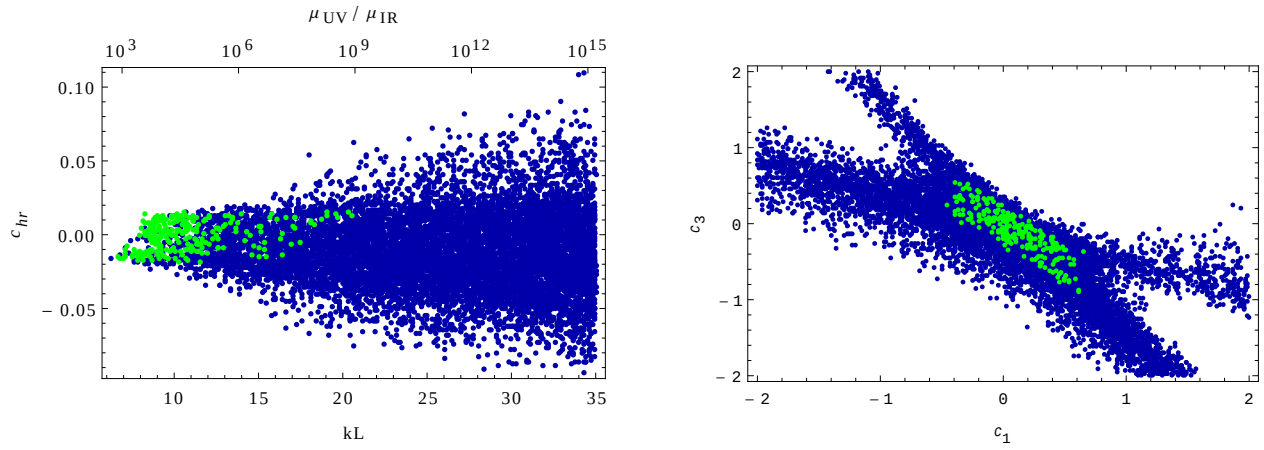

Figure 2: Results of the Λ_r, kL, c_1, c_3 parameter scan. All points shown satisfy the constraints from resonance searches and Higgs measurements, while the green points are additionally consistent with the diphoton excess. We have taken the cross section for the diphoton excess to be the weighted average of Eqs. (10) and (11), giving $4.9 \pm 1.3\,\text{fb}$.

stronger constraint. The bound on the mixing is therefore weaker at large kL and large Λ_r, where the radion production cross section is reduced. Furthermore, the points consistent with the diphoton excess (green points) are concentrated at small kL where the radion branching ratio to photons is enhanced and moreover the mixing is more strongly constrained from the massive diboson searches.

In the $v_{ew}/\Lambda_r \ll 1$ limit, c_{hr} is given in terms of the Lagrangian parameters by

$$c_{hr} = (c_1 + c_3)\,\frac{m_r^2}{m_r^2 - m_h^2}\,\frac{v_{ew}}{\Lambda_r} + \mathcal{O}\left((v_{ew}/\Lambda_r)^3\right)\,, \tag{13}$$

and hence the heavier state is strongly radion-like along the line[6] $c_1 = -c_3$, which we refer to as the alignment case. This is evident in the right panel of Figure 2 where the allowed points are all located along the diagonal. Notice that there are no allowed points with $c_1 \approx -c_3$ at large values of c_1. This region of parameter space is excluded by hh resonance searches due to the enhanced radion coupling to hh (see Table 1). Enhancing the coupling to hh also results in a decreased branching ratio to photons, hence the points satisfying the diphoton excess are concentrated around small values of c_1. These points are also aligned along the diagonal; the off-diagonal points corresponding to increased mixing generally have larger values of kL, again suppressing the branching ratio to photons.

It is clear that current experimental constraints impose small Higgs-radion mixing. Providing an explanation for the diphoton excess additionally restricts us to the region where $|c_1| \lesssim 0.5$ and requires that we be quite close to the alignment case. Hence we now restrict ourselves to the

[6]The lighter state is not necessarily strongly Higgs-like for $c_1 = -c_3$ due to the non-unitary transformation. That is instead determined by $|c_{rh}| = \frac{c_1 m_h^2 + c_3 m_r^2}{m_h^2 - m_r^2}\frac{v_{ew}}{\Lambda_r} + \mathcal{O}((v_{ew}/\Lambda_r)^3)$, where $c_{rh} = 0$ corresponds to a purely Higgs-like state.

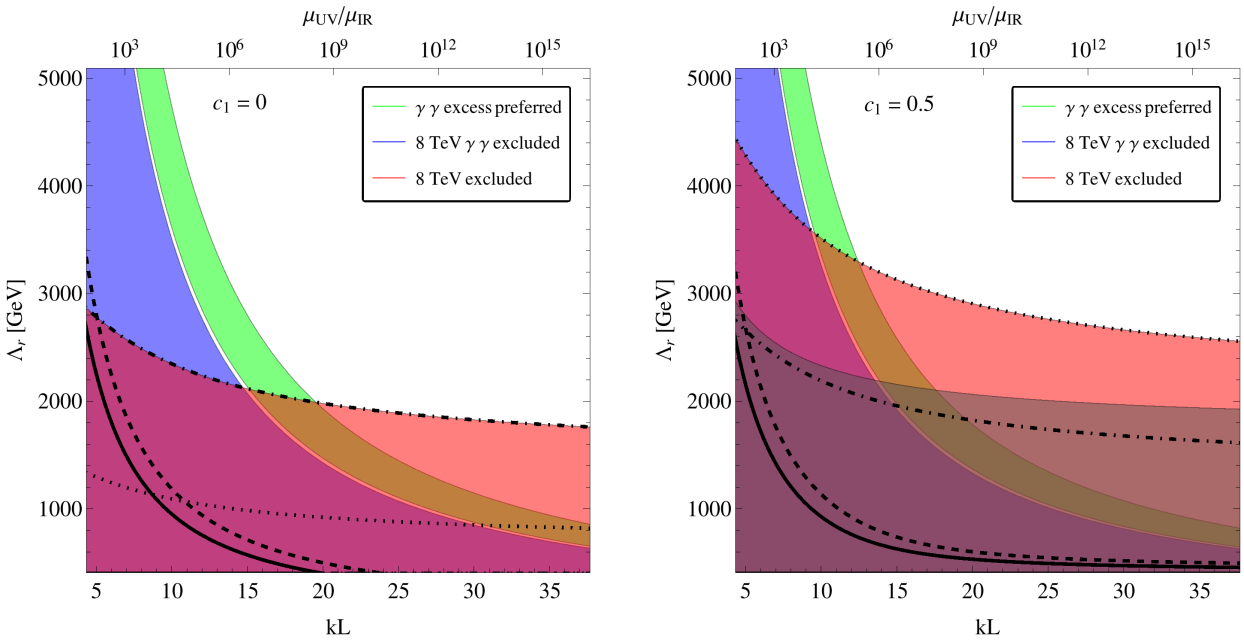

Figure 3: The region of parameter space consistent with the observed diphoton excess is shaded in green, while the blue and red regions are excluded by the 8 TeV diphoton and other resonance searches respectively, and the grey region is excluded by Higgs measurements. Regions below and to the left of the solid, dashed, dotted and dot-dashed lines are individually excluded by the WW, ZZ, hh and tt searches listed in Table 2. The left (right) panels are for $c_1 = c_3 = 0$ ($c_1 = -c_3 = 0.5$).

case $c_1 = -c_3$ in order to explore the (kL, Λ_r) parameter space in detail. In Figure 3 we show the regions in the kL–Λ_r plane consistent with the observed di-photon excess while remaining unconstrained from other LHC searches. We have taken two benchmark points corresponding to $c_1 = 0$ and $c_1 = 0.5$.

Focusing on the left panel of Figure 3 ($c_1 = 0$), we see that $t\bar{t}$ searches give the approximate bound $\Lambda_r \gtrsim 2$ TeV, while obtaining a sufficiently large diphoton signal requires taking smaller values of $kL \lesssim 20$ than those used to obtain the Planck-electroweak hierarchy in RS-models ($kL \sim 35$). This can be understood by noting that to simultaneously have a 6 fb diphoton signal at 13 TeV while avoiding the constraints from ditop searches, we must have

$$\frac{\mathcal{B}(r \to t\bar{t})}{\mathcal{B}(r \to \gamma\gamma)} < \frac{300}{6} \times \frac{\sigma(pp \to r)_{13\ \text{TeV}}}{\sigma(pp \to r)_{8\ \text{TeV}}} \approx 235\,. \tag{14}$$

As can be seen from Figure 1, this is not satisfied at $kL = 35$. Decreasing the size of the extra dimension increases the coupling to $\gamma\gamma$ (and gg, increasing the production cross section) allowing us to satisfy this constraint. In contrast, attempting to tune the mass and kinetic mixings between the radion and the Higgs to suppress the decay $r \to t\bar{t}$ while maintaining a sufficiently large production cross section reintroduces constraints from either the decays to WW or hh, as can be inferred from Figure 2.

Moving away from $c_1 = 0$ leads to an increased branching ratio to hh and this channel provides the strongest constraint for $c_1 \gtrsim 0.35$, as can be seen in the right panel of Figure 3. Satisfying this constraint in addition to the diphoton excess then requires even smaller values of kL. Also note that while the heavier state is radion-like when $c_1 = -c_3$, the lighter state is not necessarily Higgs-like due to the non-unitary transformation arising from the kinetic mixing. This leads to bounds from measurements of the Higgs couplings, which exclude the region $\Lambda_r \lesssim 2\,\text{TeV}$. However the strongest constraint still comes from the diHiggs searches, which in the particular case of $c_1 = 0.5$ push the scale $\Lambda_r \gtrsim 3.5$ TeV.

Let us briefly comment on the theoretical implications of a reduced value for kL. Models with smaller warping factors have previously been considered in the "Little Randall-Sundrum" paradigm for flavour [24]. They are most naturally interpreted in the 4D context, where the UV scale $\mu_{UV} = \mu_{IR}\, e^{kL} \sim \Lambda_r\, e^{kL}$ is the UV cut-off above which the physics is no longer conformal.[7] Flavour constraints typically require $\mu_{UV} > 10^3$ TeV, which is satisfied for all points we show in Figure 3.

Finally we address future prospects for testing this model. From Figure 1, we see that the dominant decay mode of the radion is to $t\bar{t}$ and gg. While it might be difficult to observe the di-jet final state at early runs, the possibility to explore this scenario with the di-top final state is certainly within the reach of the LHC run 2. When mixing is allowed it is clear that searches involving massive gauge boson final states will be the main tool in constraining/discovering these kinds of models. However in the particular alignment case $c_1 \approx -c_3$, where the heavier eigenstate is strongly radion-like, an interesting situation may arise in which, due to the linear c_1 dependence of the radion-diHiggs coupling, searches in the di-Higgs final state become the best way to probe the model for $c_1 \gtrsim 0.35$. We should make clear that both the diboson and the di-Higgs searches are more model dependent whereas the di-top signature is relatively insensitive to assumptions about the mixing and thus a particularly promising channel. Additionally, we note that the width of the radion is quite small, $\Gamma \lesssim 1$ GeV. If ATLAS is correct that the excess is generated by a broad resonance, that would disfavour this model as a possible explanation. However it is too soon yet to say anything concrete regarding the width and CMS seems to slightly favour a narrower resonance. Lastly, we have worked in the 4D effective theory of Eq. (6), but in the full theory we expect additional resonances at masses of a few TeV. If these are not too heavy, they might also be discoverable.

4 Conclusion

In this work we have shown that the radion in the bulk Higgs warped extra dimensional scenario can offer an explanation of the recently-observed diphoton excess at 750 GeV. The crucial observation is that the radion coupling to gauge bosons is suppressed compared to the more common brane Higgs models. This allows us to avoid the quite stringent constraints from searches for diboson resonances, provided that the mixing between the radion and the Higgs is small.

[7] For a 5D interpretation, see Ref. [25].

We find that we can match the observed excess while avoiding all 8 TeV searches for a compositeness scale $\Lambda_r \gtrsim 2$ TeV and an extra dimension of size $kL \lesssim 20$. This relatively small kL is necessary to enhance the radion coupling to diphotons. The dominant decay modes of the radion are to $t\bar{t}$ and gg, with the former providing both the most stringent bounds and the best prospects for probing these kinds of scenarios in a model-independent way in the immediate future. Mixing between the radion and the Higgs is already strongly constrained by WW/ZZ resonance searches, which require being near the alignment limit $c_1 = -c_3$. Finally, the radion branching ratio to hh can be enhanced in certain regions of parameter space, potentially providing an additional channel to probe this model.

Note added

At the same time of posting this work on the arXiv, a similar work appeared [26] discussing the radion as a possible solution to the diphoton excess.

Acknowledgements

ADM thanks Brando Bellazzini and Stephane Lavignac for useful discussions. TSR acknowledges the ISIRD Grant, IIT Kharagpur, India. This work was supported by IBS under the project code, IBS-R018-D1. This work has been supported in part by the European Research Council (ERC) Advanced Grant Higgs@LHC. This work was supported by the Australian Research Council.

References

[1] M. Kado, "ATLAS results" Talk at ATLAS and CMS physics results from Run 2, CERN, Switzerland, December 15 (2015); ATLAS Collaboration, "Search for new physics decaying to two photons," ATLAS-CONF-2015-081.

[2] J. Olsen, "CMS results," Talk at ATLAS and CMS physics results from Run 2, CERN, Switzerland, December 15 (2015); CMS Collaboration, "Search for new physics in high mass diphoton events in proton-proton collisions at 13 TeV," CMS-PAS-EXO-15-004.

[3] D. Buttazzo, A. Greljo and D. Marzocca, arXiv:1512.04929 [hep-ph].

[4] K. Harigaya and Y. Nomura, arXiv:1512.04850 [hep-ph], Y. Mambrini, G. Arcadi and A. Djouadi, arXiv:1512.04913 [hep-ph], M. Backovic, A. Mariotti and D. Redigolo, arXiv:1512.04917 [hep-ph], A. Angelescu, A. Djouadi and G. Moreau, arXiv:1512.04921 [hep-ph], Y. Nakai, R. Sato and K. Tobioka, arXiv:1512.04924 [hep-ph], S. Knapen, T. Melia, M. Papucci and K. Zurek, arXiv:1512.04928 [hep-ph], A. Pilaftsis,

arXiv:1512.04931 [hep-ph], S. Di Chiara, L. Marzola and M. Raidal, arXiv:1512.04939 [hep-ph], T. Higaki, K. S. Jeong, N. Kitajima and F. Takahashi, arXiv:1512.05295 [hep-ph], S. D. McDermott, P. Meade and H. Ramani, arXiv:1512.05326 [hep-ph], J. Ellis, S. A. R. Ellis, J. Quevillon, V. Sanz and T. You, arXiv:1512.05327 [hep-ph], M. Low, A. Tesi and L. T. Wang, arXiv:1512.05328 [hep-ph], B. Bellazzini, R. Franceschini, F. Sala and J. Serra, arXiv:1512.05330 [hep-ph], R. S. Gupta, S. Jger, Y. Kats, G. Perez and E. Stamou, arXiv:1512.05332 [hep-ph], C. Petersson and R. Torre, arXiv:1512.05333 [hep-ph], E. Molinaro, F. Sannino and N. Vignaroli, arXiv:1512.05334 [hep-ph], R. Franceschini *et al.*, arXiv:1512.04933 [hep-ph], A. Kobakhidze, F. Wang, L. Wu, J. M. Yang and M. Zhang, arXiv:1512.05585 [hep-ph].

[5] L. Randall and R. Sundrum, Phys. Rev. Lett. **83**, 3370 (1999) [hep-ph/9905221].

[6] P. Cox, A. D. Medina, T. S. Ray and A. Spray, JHEP **1402** (2014) 032 [arXiv:1311.3663 [hep-ph]].

[7] O. DeWolfe, D. Z. Freedman, S. S. Gubser and A. Karch, Phys. Rev. D **62**, 046008 (2000) [hep-th/9909134].

[8] B. Bellazzini, C. Csaki, J. Hubisz, J. Serra and J. Terning, Eur. Phys. J. C **74**, 2790 (2014) [arXiv:1305.3919 [hep-th]], F. Coradeschi, P. Lodone, D. Pappadopulo, R. Rattazzi and L. Vitale, JHEP **1311**, 057 (2013) [arXiv:1306.4601 [hep-th]], E. Megias and O. Pujolas, JHEP **1408**, 081 (2014) [arXiv:1401.4998 [hep-th]], P. Cox and T. Gherghetta, JHEP **1502**, 006 (2015) [arXiv:1411.1732 [hep-th]].

[9] C. Csaki, J. Hubisz and S. J. Lee, Phys. Rev. D **76**, 125015 (2007) [arXiv:0705.3844 [hep-ph]].

[10] CMS Collaboration, CMS-PAS-EXO-16-018.

[11] S. Chatrchyan *et al.* [CMS Collaboration], arXiv:1309.2030 [hep-ex].

[12] V. Khachatryan *et al.* [CMS Collaboration], JHEP **1510**, 144 (2015) [arXiv:1504.00936 [hep-ex]].

[13] G. Aad *et al.* [ATLAS Collaboration], arXiv:1509.00389 [hep-ex].

[14] G. Aad *et al.* [ATLAS Collaboration], arXiv:1507.05930 [hep-ex].

[15] G. Aad *et al.* [ATLAS Collaboration], Phys. Lett. B **738**, 428 (2014) [arXiv:1407.8150 [hep-ex]].

[16] CMS Collaboration, CMS-PAS-HIG-16-014.

[17] G. Aad *et al.* [ATLAS Collaboration], Phys. Rev. D **92**, no. 3, 032004 (2015) [arXiv:1504.05511 [hep-ex]].

[18] V. Khachatryan *et al.* [CMS Collaboration], Phys. Lett. B **750**, 494 (2015) [arXiv:1506.02301 [hep-ex]].

[19] G. Aad *et al.* [ATLAS Collaboration], Phys. Rev. D **92**, 092004 (2015) [arXiv:1509.04670 [hep-ex]].

[20] G. Aad *et al.* [ATLAS Collaboration], Phys. Rev. D **91** (2015) 5, 052007 [arXiv:1407.1376 [hep-ex]].

[21] CMS Collaboration, CMS-PAS-EXO-14-005.

[22] S. Heinemeyer *et al.* [LHC Higgs Cross Section Working Group Collaboration], arXiv:1307.1347 [hep-ph].

[23] The ATLAS and CMS Collaborations, ATLAS-CONF-2015-044.

[24] H. Davoudiasl, G. Perez and A. Soni, Phys. Lett. B **665**, 67 (2008) [arXiv:0802.0203 [hep-ph]].

[25] D. P. George and K. L. McDonald, Phys. Rev. D **84**, 064007 (2011) [arXiv:1107.0755 [hep-ph]].

[26] A. Ahmed, B. M. Dillon, B. Grzadkowski, J. F. Gunion and Y. Jiang, arXiv:1512.05771 [hep-ph].